Short Papers

Modeling of Microwave Top Illuminated PIN Photodetector Under Very High Optical Power

J. Harari, G. H. Jin, F. Journet, J. Vandecasteele,
J. P. Vilcot, C. Dalle, M. R. Friscourt, and D. Decoster

Abstract— **In this paper, we present a theoretical study and a numerical simulation of a classical long wavelength top illuminated PIN photodetector for microwave applications under very high optical power. The modeling includes a monodimensional drift-diffusion model for the device and takes into account the external circuit. At first, this modeling is validated using experimental results from the literature. Second, we consider a classical InP/GaInAs/InP photodiode grown on N^+ InP substrate. The presented results show that the distortion and the saturation of the microwave signal at 20 GHz are due to the space charge effect in the photodetector and also to the depolarization of the device because of the external circuit. The main parameter influencing these phenomena are the optical power, the bias voltage, the optical spot width and the modulation depth. In case of small optical spot, the effect of the external circuit is neglectable, while it contributes to the decrease of the microwave responsivity in case of large spot. The maximum output power is calculated in different cases and we can expect up to 12 dBm microwave output power for a 5 V reverse bias voltage.**

I. Introduction

The improvements of optical fiber links performance make now possible to transmit microwave signals through an optical fiber. This leads to new applications such as antenna remoting, phase array antenna, etc. for which the transmission of high power microwave signals could simplify the systems. In this field, the behavior of photodetectors under high optical power is important. Since 1988, a lot of work has been made concerning top illuminated photodiodes [1]–[6], MSM photodetectors [7], and waveguide PIN photodetectors [8]–[10]. However, the effects of external circuit has not been taken into account. Moreover, the maximum microwave power which can be obtained from this type of photodetector has not been clearly defined, neither experimentally nor theoretically. This is the reason we present a simulation of the behavior of a classical top illuminated PIN photodiode under high optical signal taking into account the external circuit.

II. Modeling

A monodimensional drift-diffusion model had demonstrated its capabilities in comparison with energy model in Si and GaAs IMPATT diodes [11]. This was used to analyze our classical InP/GaInAs/InP photodiode. The external circuit was introduced as a relation between the diode voltage v_d and the diode photocurrent i_d. The whole simulated circuit is presented in Fig. 1. The bias tee composed of a capacitor and an inductor ($C_1 = 1.6$ nF, $L_2 = 40$ nH) allows a good filtering at 20 GHz conditions. The resistor $R_2 (R_2 = 2\ \Omega)$ is those of the dc voltage generator. The equations representing this

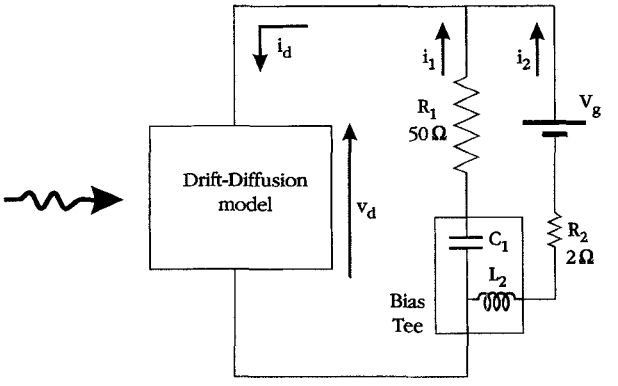

Fig. 1. Whole circuit introduced in the numerical simulation.

circuit are

$$v_d = \frac{1}{C_1}\int i_1 \cdot dt + R_1 i_1$$
$$v_d = L_2 \frac{di_2}{dt} + R_2 i_2 + V_g$$
$$i_d = i_1 + i_2$$

where v_d is the diode voltage, i_d the photocurrent and V_g the dc bias voltage. The resistor R_1 represents the microwave load ($R_1 = 50\ \Omega$). Considering now the simulated photodetector, the GaInAs N^- absorbing layer is 1.5 μm thick and its doping level is 10^{15} cm^{-3}. The InP P^+ and N^+ epilayer doping levels are 10^{18} cm^{-3}. The P^+/N^- junction is located at the InP/GaInAs heterointerface. The photodetector surface is 400 μm^2 to insure negligible capacitance effect. Under small signal conditions, the calculated cut-off frequency is equal to 22 GHz and the responsivity to 0.8 A/W, in case of anti-reflection coating on the top of the photodiode (otherway, the optical reflection coefficient at the top of the device is 29%, and the responsivity decreases down to 0.57A/W). Carrier mobilities have been taken in [1], [10]. The comparison with experimental results drove us to choose different values of mobility in GaInAs and in InP as we will see in the next section. Valence and conduction band discontinuities between InP and GaInAs are from [13].

In this work, we neglect the effects of temperature and we assume that the hole and electron densities in the material are not sufficiently high to modify the absorption coefficient of GaInAs ($\alpha = 0.68\ \mu$m^{-1} at $\lambda = 1.55\ \mu$m). The input optical signal introduced has the following form:

$$P_L(t) = P_{L0}(1 + m\cos(2\pi f t)).$$

The frequency f used in the calculations is 20 GHz, slightly under the cut-off frequency of the PIN photodetector. We made successively a temporal response of the device in its circuit, and a Fourier Transform to get the contribution of the different harmonics in the electrical output signal. The bias voltage introduced are -2 and -5 V. Moreover, because the optical spot width is an important factor, we considered different spot widths.

Manuscript received July 1, 1994; revised April 19, 1996.

The authors are with the Institut d'Electronique et de Microélectronique du Nord, UMR CNRS 9929. DHS, 59652 Villeneuve d'Ascq Cedex, France.

Publisher Item Identifier S 0018-9480(96)05639-6.

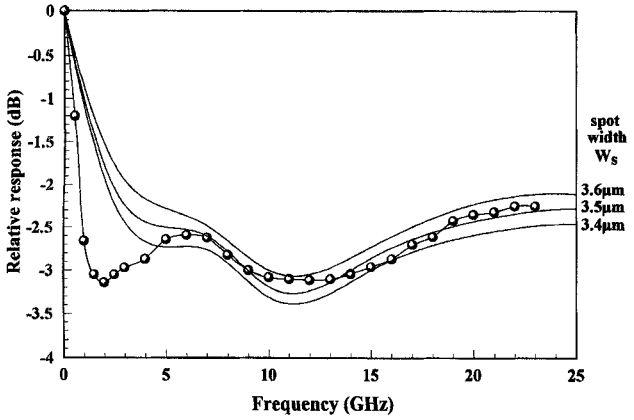

Fig. 2. Comparison with experimental results. Frequency response of the photodetector PD1 of [5] at 1 mA (modulation depth: 10%) relative to response at 100 μA (modulation depth: 100%). The pointed line is the experimental result.

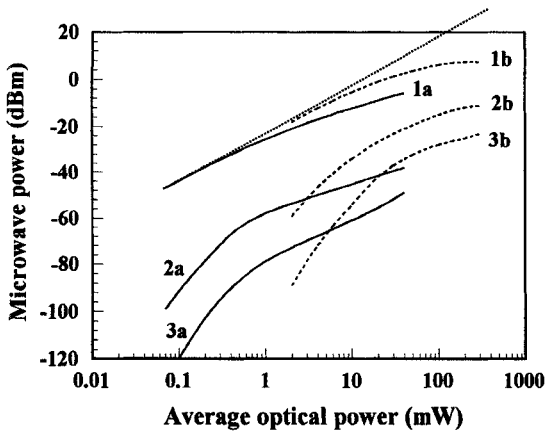

Fig. 3. Microwave response of the typical structure at 20 Ghz. The modulation depth is 100%. 1. Fundamental, 2 and 3 harmonics of order two and three. The straight line represents a constant responsivity. a) $V_g = -2$ V, $W_s = 4$ μm; b) $V_g = -2$ V, $W_s = 16$ μm.

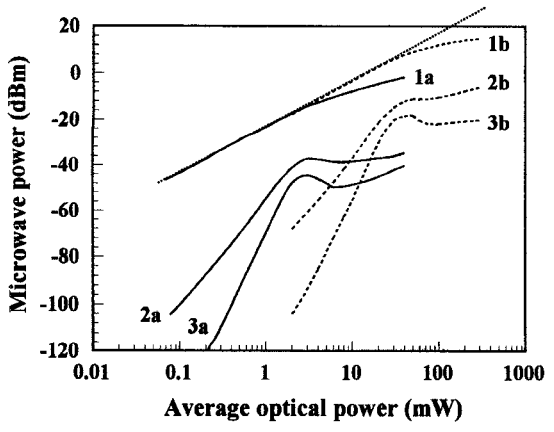

Fig. 4. Microwave response of the typical structure at 20 Ghz. The modulation depth is 100%. 1. Fundamental, 2 and 3 harmonics of order two and three. The straight line represents a constant responsivity. a) $V_g = -5$ V, $W_s = 4$ μm; b) $V_g = -5$ V, $W_s = 16$ μm.

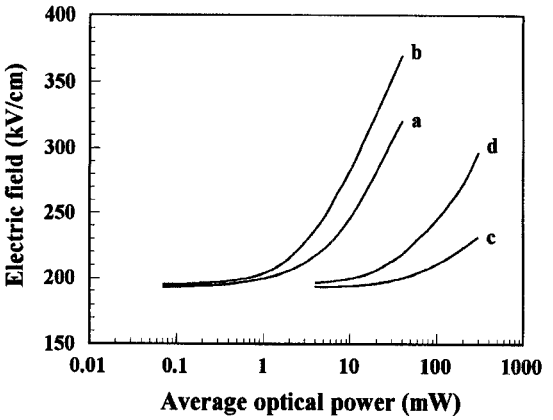

Fig. 5. Maximum electric field at the P^+/N^- heterointerface versus average optical power. a) $V_g = -2$ V, $W_s = 4$ μm, b) $V_g = -5$ V, $W_s = 4$ μm, c) $V_g = -2$ V, $W_s = 16$ μm, d) $V_g = -5$ V, $W_s = 16$ μm.

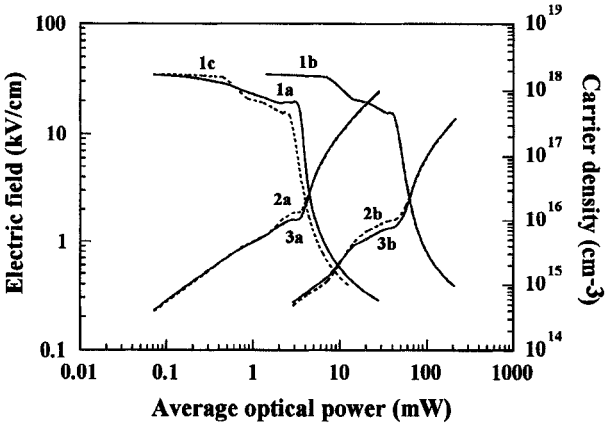

Fig. 6. Electric field and carrier densities at the center of the depletion region versus average optical power. 1a) electric field: $V_g = -5$ V, $W_s = 4$ μm. 1b) Electric field: $V_g = -5$ V, $W_s = 16$ μm. 1c) Same as 1b) but shifted toward left with a scale factor of 16. 2a) and 3a), respectively, holes and electrons: $V_g = -5$ V, $W_s = 4$ μm. 2b) and 3b), respectively, holes and electrons: $V_g = -5$ V, $W_s = 16$ μm.

III. Results

A. Comparison with Experimental Results

The accuracy of our numerical simulation was tested with the experimental results given by Williams *et al.* [5] for the same photodiode structure [14] and modulated optical illuminations (spot size 5.75 μm). The mobilities used in our calculations follow the law given by Dentan et al [1] and the best results have been obtained for electron and hole mobility of 10500 cm^2/V· s and 420 cm^2/V· s, respectively, in GaInAs N^-. Different values have been taken in InP and GaInAs P^+,, respectively, (3500 cm^2/V · s, 150 cm^2/V· s) and (3000 cm^2/V · s, 130 cm^2/V · s) [12]. The value of the electron and hole life time in N^- GaInAs is equal to 10^{-8} s, and we introduced the GaInAs N^-/InP N heterointerface. Our results, given in Fig. 2, are close to those obtained theoretically by Williams *et al.* [5]; the small spot width induces high carrier densities inside the device and a small external photocurrent, the depolarization effect is so negligible. In comparison with the experimental results, the best fit corresponds to an equivalent spot width of 3.5 μm which is a little bit higher than the theoretical one (3 μm) suggested by Williams *et al.* The discrepancy between experimental and theoretical values is due to the

TABLE I
PERFORMANCE OF THE PHOTODETECTOR AT 20 GHz, FOR EACH BIAS VOLTAGE, SUCCESSIVELY THE AVERAGE OPTICAL POWER P_{opt}, THE CORRESPONDING MICROWAVE POWER P_m, AND THE LOSS OF RESPONSIVITY Δ_r COMPARED WITH THE SMALL SIGNAL RESPONSIVITY

Bias voltage	-2V			-5V		
Spot width	P_{opt}	P_m	Δr	P_{opt}	P_m	Δr
4μm	10mW	-14dBm	-10dB	6mW	-10dBm	-3dB
16μm	300mW	+7dBm	-22dB	100mW	+12dBm	-8dB

fact that the monodimensional modeling does not take into account the realistic optical power distribution of the spot.

B. Theoretical Study and Results

The photodiode structure is the one described in Section II. We considered two different spot widths W_s: 4 μm and 16 μm. The first corresponds to a typical spot size obtained with a lensed fiber [5], the second to the typical size obtained with a cleaved monomode fiber at 1.55 μm (Corning SMF-9-125 for example). For all presented results, the value of the optical power takes into account a reflexion coefficient of 0.29 at the top of the photodiode. The microwave response of the photodetector with its external circuit is represented for bias voltages of -2 V and -5 V, respectively, in Figs. 3 and 4. We can observe that the harmonic level is higher at -2 V than at -5 V because of the smaller electric field in the depletion region in the first case. When a high optical modulated signal is applied, there is a redistribution of electric field in the device. This field decreases in the middle of the depletion region and increases at the P^+/N^- heterointerface. So the maximum electric field is located at the P^+/N^- heterointerface, its evolution for each microwave response versus optical power is presented in Fig. 5. It can exceed 250 kV/cm for high optical power. For this value and above, the band to band tunneling effect becomes important in the GaInAs layer [15], which introduces a parasitic current making the breakdown possible. Because the heterointerface electric field changes with the instantaneous carrier densities present in the photodetector, the parasitic current will be modulated with an average value which leads to a breakdown phenomenon in GaInAs [15]. This is the reason why we interrupted the simulations for higher average optical power. As a consequence, by increasing the reverse bias voltage, we decrease the harmonic in the microwave signal but increase the maximum electric field at the P^+/N^- heterointerface. So, the bias voltage must be a trade off to get the highest microwave output power while avoiding tunneling current.

Considering now the influence of the optical spot size, for the same average optical power, the optical power density applied on the photodetector is 16 times less for a 16 μm spot width than for a 4 μm one. If the external circuit is not taken into account, the curves a and b of Fig. 3 (or 4 for example) ought to be the same with only a shift of optical power scale by a factor 16. But their differences make the influence of the external circuit appear. Particularly, the decrease of the responsivity with increasing optical power is more important. This difference is explained by the depolarization of the photodiode by the instantaneous voltage drop due to the microwave load (50 Ω resistor). The Fig. 6 presents the variation of the electric field and carrier densities at the center of the depletion region versus optical power for a bias voltages of -5 V and for different spot width. In this Figure, we have shifted the curve corresponding to a 16 μm spot size [curve 1b)] to the left with a scale factor of 16 [curve 1c)]. Without external circuit, the two curves corresponding to 4 μm and 16 μm spot sizes, ought to be exactly parallel, so the curves 1a and 1c ought to be exactly the same. The difference which can be observed is due to external circuit which decreases the electric field more. Our results show that this effect of depolarization is less important at -5 V than at -2 V. This is due to the fact that the electric field in the depletion region is smaller in the second case, so the depolarization effect has more importance. Finally, concerning the electron and hole carrier densities [curves 2a), 3a), 2b), 3b)] three zones can be distinguished; 1) the first, where the electric field is high and the densities increase linearly with optical power, then, the microwave responsivity is constant; 2) the second, where the electric field decreases quickly and the carrier densities increase quicker than before with optical power, then, the microwave responsivity decreases; 3) the third, where the electric field decreases more and the carrier densities increase with a slope lower than in the second zone, then, the responsivity decreases strongly. If we limit the maximum P^+/N^- heterointerface electric field at 250 kV/cm, the performances of this photodetector are summarized in Table I. Larger spot widths will yield in higher optical power withstanding as well as microwave delivered powers. Higher bias voltage can confer the responsivity a more linear behavior versus impinging optical power.

IV. CONCLUSION

We presented a modeling of microwave PIN photodetectors based on a mono-dimensional Drift-Diffusion model and taking into account the external circuit. First, we compared the theoretical results given by our simulation with experimental ones, which gave good accuracy. Second, we presented the behavior of a classical InP/GaInAs/InP heterostructure with cut-off frequency of 22 GHz in small signal conditions. The study at 20 GHz, for two bias voltages -2 and -5 V, and for two spot widths 4 and 16 μm, demonstrated the necessity to apply a high reverse bias voltage but not too high in order to avoid breakdown due to band to band tunneling effect at the P^+/N^- heterointerface. The results also demonstrate the importance of a large spot width in order to decrease the optical power density in the device for a same input optical power. For small spot size, the external circuit has a very small influence since intrinsic phenomena limit the performance of the device before external circuit effect occurs, but for an illumination through a typical monomode fiber, the influence of this circuit can be observed. Anyway, the number of parameters which influence the behavior of such a photodetector under high modulated optical power is important. We can point out the bias voltage, the optical spot width, the device structure with its heterointerfaces, and also the modulation depth of the input optical signal as demonstrated by our comparison between experiments and theory. The illumination conditions are important, which is uneasy to control exactly during experiments. The main performances theoretically obtained with the simulated structure are a maximum microwave power of about ten dBm (+12 dBm at -5 V for a spot size of 16 μm). This maximum microwave power can be obtained at -5 V with a responsivity 8 dB lower than the small signal responsivity, and at -2 V with a loss of responsivity of 22 dB. This makes necessary to applied 100 mW at -5 V and 300 mW at -2 V.

REFERENCES

[1] M. Dentan and B. de Cremoux, "Numerical simulation of the nonlinear response of a PIN photodiode under high illumination," *J. Lightwave Technol.*, vol. 8, pp 1137–1144, 1990.

[2] R. D. Esman and K. J. Williams, "Measurement of harmonic distortion in microwave photodetectors," *IEEE Photon. Technol. Lett.*, vol. 2, no. 7, pp. 502–504, 1990.

[3] K. J. Williams and R. D. Esman, "Observation of photodetector nonlinearities," *Electron. Lett.*, vol. 28, no. 8, pp. 731–733, 1992.

[4] R. R. Hayes and D. L. Persechini, "Nonlinearity of PIN photodetectors," *IEEE Photon. Technol. Lett.*, vol. 5, no. 1, pp. 70–72, 1993.

[5] K. J. Williams, R. D. Esman, and M. Dagenais, "Effect of high space-charge fields on the response of microwwave photodetectors," *IEEE Photon. Technol. Lett.*, vol. 6, no. 5, pp. 639–641, 1994.

[6] K. J. Williams, "Nonlinear mechanisms in microwave photodetectors operated with high intrinsic region electric fields," *Appl. Phys. Lett.* vol. 65, no. 10, pp. 1219–1221, 1992.

[7] I. S. Ashour, J. Harari, J. P. Vilcot, and D. Decoster, "High optical power nonlinear dynamic response of AlInAs/GaInAs MSM photodiode," *IEEE Trans. Electron Devices*, vol. 42, no. 5, pp. 828–834, 1995.

[8] A. R. Williams, A. L. Kellner, A. L. Jiang, and P. K. L. Yu, "InGaAs/InP waveguide photodetector with high saturation intensity," *Electron. Lett.*, vol. 28, no. 24, pp. 2258–2259, 1992.

[9] A. R. Williams, A. L. Kellner, and P. K. L. Yu, "High frequency saturation measurements of an InGaAs/InP waveguide photodetector," *Electron. Lett.*, vol. 29, no. 14, pp. 1298–1299, 1993.

[10] D. Wake, N. G. Walker, and I. C. Smith, "Zero-bias edge coupled InGaAs photodiodes in millimeter wave radio fiber systems," *Electron. Lett.*, vol. 29, no. 21. pp. 1879–1881, 1993.

[11] C. Dalle and P. A. Rolland, "Drift-diffusion versus energy model for millimeter wave IMPATT diodes modeling," *Int. J. Numerical Modeling: Electronic Networks, Devices and Fields*, vol. 2, no. 1, pp. 61–73, 1989.

[12] T. P. Pearsall, *GaInAsP alloy semiconductors.* New York: Wiley, 1982.

[13] S. R. Forrest, P. H. Schmidt, R. B. Wilson, and L. Kaplan, "Relationship between the conduction band discontinuities and bandgap differences in InGaAsP/InP heterojunctions," *Appl. Phys. Lett.*, vol. 45, no. 8, pp. 1199–1202, 1984.

[14] J. Schlafer, C. B. Su, W. Powazinik, and R. B. Lauer, "20 GHz bandwidth InGaAs photodetector for long wavelength microwave optical links," *Electron. Lett.*, vol. 21, no. 11, pp. 469–471, 1985.

[15] J. Harari, D. Decoster, J. P. Vilcot, B. Kramer, C. Oguey, P. Salzac, and G. Ripoche, "Numerical simulation of avalanche photodiodes with guard ring," *IEE Proc-J*, vol. 138, no. 3, pp. 211–217, 1991.

Improvements of the Two-Dimensional FDTD Method for the Simulation of Normal- and Superconducting Planar Waveguides Using Time Series Analysis

Stefan Hofschen and Ingo Wolff

Abstract— **Time-domain simulation results of two-dimensional (2-D) planar waveguide finite-difference time-domain (FDTD) analysis are normally analyzed using Fourier transform. The introduced method of time series analysis to extract propagation and attenuation constants reduces the desired computation time drastically. Additionally, a nonequidistant discretization together with an adequate excitation technique is used to reduce the number of spatial grid points. Therefore, it is possible to simulate normal- and superconducting planar waveguide structures with very thin conductors and small dimensions, as they are used in MMIC technology. The simulation results are compared with measurements and show good agreement.**

Manuscript received September 9, 1994; revised April 19, 1996.

The authors are with the Department of Electrical Engineering, Gerhard Mercator University of Duisburg, Duisburg, Germany.

Publisher Item Identifier S 0018-9480(96)05657-8.

I. INTRODUCTION

Recently, a two-dimensional finite-difference time-domain (2-D-FDTD) algorithm has been introduced as an efficient full-wave analysis method for arbitrarily shaped waveguide structures [1]. Normally, the simulation results are extracted from the time series using Fourier transform. For very small structures and thin conductors, as they are used in the MMIC technology, a very fine spatial discretization is required. Due to the stability condition of the FDTD technique, the fine spatial discretization causes a very fine time discretization, too.

In this work we introduce a time series analysis technique using a Powell optimization technique to extract dispersion and loss characteristics of planar waveguiding structures from only a part of a single period of the time signal. Especially if the fields inside the conductors have to be calculated to analyze the waveguide losses, the method reduces the required computation time up to a factor of 25. Therefore, it is possible to simulate planar and coplanar waveguides with a metallization thickness of only 2 μm or a superconducting film thickness of 300 nm, which cannot be simulated with the conventional FDTD or 2-D-FDTD techniques due to the enormous CPU time needed.

II. THEORY

For the 2-D-FDTD algorithm, the spatial derivatives for the transverse fields in one direction, e.g., the x-direction, which should be the propagation direction of the guided wave, are replaced using the analytical formulas [1]

$$\underline{\vec{E}}_t(x \pm \Delta x) = \underline{\vec{E}}_t(x) \cdot e^{\mp \jmath \beta \Delta x}$$

$$\underline{\vec{H}}_t(x \pm \Delta x) = \underline{\vec{H}}_t(x) \cdot e^{\mp \jmath \beta \Delta x}. \tag{1}$$

Thus, 2-D-FDTD mesh formulation can be derived. During the simulation, a propagation constant β and a proper excitation are chosen. After a certain number of iterations, the corresponding modal frequencies can be extracted using Fourier transform of the time series obtained. In the conventional approach, repeating the Fourier transform after some iterations makes it possible to calculate the losses of the waveguiding structure. For the 2-D-FDTD method, a new stability condition can be derived under the assumption that $\Delta x \rightarrow 0$ [2]

$$c_0 \Delta t = \left[\frac{1}{(\Delta y)^2} + \frac{1}{(\Delta z)^2} + \left(\frac{\beta}{2} \right)^2 \right]^{-\frac{1}{2}}. \tag{2}$$

It can be seen that the time step Δt depends on the maximum wave phase velocity c_0 in the air-filled region above the dielectric substrate, and mainly on the spatial discretizations Δy and Δz. The discretizations Δy and Δz inside the conducting material should be smaller than the skin depth in the case of a normal conductor, or smaller than the London penetration depth in the case of a superconductor for the given material and frequency. Due to the extreme short corresponding time step Δt, a tremendous number of iterations is necessary to obtain the time series of voltage and current on the waveguide for at least one period. The simulations demonstrated in the following would, e.g., require at least 10^5 iteration steps for one period at 8 GHz, using a discretization of 0.5 μm. Keeping in mind that several periods are necessary for an exact Fourier transform, the simulation of such a structure becomes nearly impossible using the conventional technique. The